

Classical and quantal atomic form factors for arbitrary transitions

D. Vranceanu and M. R. Flannery

School of Physics, Georgia Institute of Technology, Atlanta, Georgia 30332

(Received 24 February 1999)

The classical form factor is deduced from exact correspondence with a phase-space representation of the quantal form factor. Analytical expressions are provided for $nl \rightarrow n'l'$, $nl \rightarrow n'$, and $n \rightarrow n'$ transitions in hydrogenic systems and for $n \rightarrow n'$ in the one-dimensional harmonic oscillator. An efficient procedure for calculation of quantal form factors as analytical functions of momentum transfer, for arbitrary quantum numbers, is presented. The classical approach has the ability to explain quite succinctly interesting trends and various important aspects which remain hidden within the quantal treatment of form factors. The classical-quantal comparison ranges from being qualitatively good for $nl \rightarrow n'l'$ transitions to close agreement for $nl \rightarrow n'$ and $n \rightarrow n'$ transitions. Excellent agreement is obtained for the integrated form factor for all transitions. [S1050-2947(99)09107-6]

PACS number(s): 32.80.Cy, 34.50.-s, 31.15.Gy

I. INTRODUCTION

The inelastic form factor

$$\mathcal{F}_{fi} = \langle \Psi_f | e^{i\mathbf{q} \cdot \mathbf{r}/\hbar} | \Psi_i \rangle = \langle \Psi_f | e^{i\mathbf{K} \cdot \mathbf{r}_{a.u.}} | \Psi_i \rangle$$

is a very basic quantity. It can accurately describe the overall response and dynamics of an atom or molecule involved in various processes or external interactions. It is also common in various schemes of approximation.

The study of the hydrogen atom form factor serves as a pivotal starting point for the general study of electronic transitions between highly excited states of atoms and molecules. The additional effects of the nonhydrogenic core may be incorporated via use of quantum defect theory. Inelastic transitions between the ro-vibrational states of molecules can be studied by appeal to the inelastic form factor for the harmonic oscillator.

Inelastic scattering of incident (neutral or charged) particles or of photons (or short bursts of electromagnetic radiation [1]) by a structured target can be decomposed into an internal structure part, provided by the form factor of the target, and a dynamic part which depends on details of the external projectile-target interaction. Bound-bound, bound-continuum, continuum-continuum, and ionization transitions are treated on the same footing by using the form factor.

Inelastic scattering of incident (neutral or charged) particles or of photons (or short bursts of electromagnetic radiation [1]) by a structured target can be decomposed into an internal structure part, provided by the form factor of the target, and a dynamic part which depends on details of the external projectile-target interaction. Bound-bound, bound-continuum, continuum-continuum, and ionization transitions are treated on the same footing by using the form factor.

The quantal impulse, semiclassical impact parameter, first Born approximation, and binary encounter methods of collision theory [2] focus on the transition probability as a dynamic response of the target in the field of the projectile. The physical significance of the form factor \mathcal{F} is that $P_{if}(\mathbf{q}) = |\mathcal{F}|^2$ is the probability of an internal transition arising from any external impulsive perturbation (whether due to collision with particles or exposure to electromagnetic radiation) which induces a sudden change \mathbf{q} to the internal momentum of the target system [3]. Since any interaction can be decomposed as a series of sudden interactions, the scattering cross section or other observables are determined by integrating the form factor, multiplied by some weighting factor characteristic of the interaction, over momentum transfer \mathbf{q} . For

example, the generalized oscillator strength f is written in terms of the inelastic form factor as

$$f = \frac{2\Delta E_{a.u.}}{K^2} |\mathcal{F}|^2,$$

where $\mathbf{K} = \mathbf{q}(a_0/\hbar)$ is dimensionless, and where $\Delta E_{a.u.}$ is the change in energy between the initial and final states. The first Born approximation for the inelastic scattering of structureless ions of charge Ze , of speed v , by a hydrogenlike ion of charge $Z'e$, is

$$\sigma(v) = \frac{8\pi ZZ' a_0^2}{(v/v_0)^2} \int_{K_{min}}^{K_{max}} |\mathcal{F}(K)|^2 K^{-3} dK,$$

which can emphasize small momentum transfers K occurring at high energies. The inelastic scattering of an ultraslow neutral particle by a Rydberg atom is

$$\sigma(v) = \frac{2\pi a^2}{(v/v_0)^2} \int_{K_{min}}^{K_{max}} |\mathcal{F}(K)|^2 K dK,$$

where a is the scattering length of the projectile-Rydberg-electron interaction and $v_0 = e^2/\hbar$ is the atomic unit for velocity. This expression emphasizes intermediate and larger K occurring within the interaction distance a .

Classical mechanics provides a good quantitative description of excited states via the correspondence principles [4]. Classical mechanics also promotes physical insight into the process by transparent causality, and provides scaling laws and elucidation of the dynamics. A phase-space description combined with statistical properties (microcanonical distribution in most cases) are the basis for an alternative or complementary view of quantal phenomena.

Based on the recognition of the above fundamental aspects of the form factor, this paper presents results for quantal form factors, and defines the classical form factor for the highly excited hydrogen atom and harmonic oscillator. Classical mechanics is advantageous here (a) in revealing essential details of the dynamics for inelastic transitions, (b) in

explaining the interesting trends in the behavior of the form factor (as a function of the various variables), and (c) in predicting quantitative results inaccessible to rigorous quantal calculations because of the formidable numerical restrictions imposed by the highly oscillatory wave functions.

Some analytical quantal [5,6], semiclassical [7,8] and classical [9,6] form factors are available, but general systematic trends cannot be easily extracted from them. A key point of this paper is that a complementary classical approach for general $nl \rightarrow n'l'$ transitions is developed in such a way that reveals quite succinctly important aspects which remain hidden within the quantal treatment. The consistency of this approach is verified by applying it to $nl \rightarrow n'$ and $n \rightarrow n'$ transitions. The known results [6] are then rederived in a unified way.

The simple example of the one-dimensional harmonic oscillator is treated in Sec. II. The correspondence between the quantal and classical form factor for inelastic transitions in this system is apparent. On this ground, a generalization for three-dimensional systems (like the hydrogen atom) becomes feasible. A definition of the classical form factor interpreted as a transition probability between two states described by microcanonical distributions in the phase space, is proposed in Sec. III. The classical form factor for $nl \rightarrow n'l'$ is introduced in Sec. IV, and compared with the quantal counterpart. Various summations, over the momentum transfer and initial and final quantum numbers are obtained within the same theoretical framework. The classical calculation are based on the microcanonical distributions presented in Appendix A. In Appendix B the classical calculations are detailed. An efficient algorithm for calculation of the various quantal form factors is introduced in Appendix C.

II. FORM FACTOR FOR THE HARMONIC OSCILLATOR

The simple example of the one-dimensional harmonic oscillator with the Hamiltonian

$$H = p^2/2m + m\omega^2 r^2/2$$

is considered in this section. The quantized energy levels are $E_n = (n + 1/2)\hbar\omega$, and the corresponding wave functions $u_n(r)$ have the generating function

$$F(t, r) = \sum_{n=0}^{\infty} \frac{u_n(r)t^n}{\sqrt{n!}} = \pi^{-1/4} r_0^{-1/2} \times \exp[-(r/r_0)^2/2 + \sqrt{2}tr/r_0 - t^2/2],$$

where $r_0 = \sqrt{\hbar/m\omega}$ is the natural length of the oscillator.

The inelastic form factor for the transition from level n to level n' when the momentum q is transferred is defined as

$$\mathcal{F}_{nn'}(q) = \langle u_{n'} | e^{iqr/\hbar} | u_n \rangle,$$

and has the generating function, in terms of the dimensionless variable $Q = qr_0/\sqrt{2}\hbar$

$$I(t, z; Q) = \sum_{n,m=0}^{\infty} \mathcal{F}_{nn'} \frac{t^n z^m}{\sqrt{n!m!}} = \exp(-Q^2/2) \exp[tz + i(t+z)Q].$$

This function provides an easy way to compute the form factor by using

$$\mathcal{F}_{nn'} = \frac{1}{\sqrt{n!n'!}} \left. \frac{\partial^{n+n'} I(t, z; Q)}{\partial^n t \partial^{n'} z} \right|_{t,z=0}, \quad (1)$$

and reveals the following analytical structure of the quantal form factor for the harmonic oscillator:

$$\mathcal{F}_{nn'} = \exp(-Q^2/2) W_{n+n'}(Q),$$

where $W_{n+n'}$ is a polynomial of order $n+n'$.

The square of the absolute value of the form factor can be interpreted as the transition probability of the harmonic oscillator when an impulsive interaction imparts momentum q [3]. Based on this observation, a classical analog of the form factor can be defined. Consider the phase space to be populated according to the microcanonical distribution. The transition probability is then given, in a geometric sense, by the volume of that region in phase space where both initial and final states can coexist.

The density of probability in phase space for a given state of the harmonic oscillator is

$$\rho_n(r, p) = N \delta(H(r, p) - (n + \frac{1}{2})\hbar\omega),$$

where the normalization factor $N = \omega/2\pi$ ensures one particle in all of the phase space. The transition probability is then given by the conditional probability that the the system in the initial state n is in the phase-space volume element $dr dp$, and the q -displaced final state has quantum number n' within the same volume element. Hence

$$P_{nn'}(q) = \frac{\hbar\omega^2}{2\pi} \int dr dp \delta(H(r, p) - (n + \frac{1}{2})\hbar\omega) \times \delta(H(r, p+q) - (n' + \frac{1}{2})\hbar\omega)$$

Phase space integration yields

$$P_{nn'}(Q) = \frac{1}{\pi} [-Q^4 + 2(n+n'+1)Q^2 - (n-n')^2]^{-1/2}, \quad (2)$$

where the dimensionless parameter $Q^2 = (q^2/2m)/\hbar\omega$ is, again, $q^2 r_0^2 / 2\hbar^2$. Then

$$P_{nn'}(Q) = \frac{1}{\pi} [(Q_+^2 - Q^2)(Q^2 - Q_-^2)]^{-1/2},$$

which shows that q is restricted to those values for which the square root is a real number; otherwise the transition is classically forbidden, and $P_{nn'}$ is zero. The limiting values of $Q = Q_{\pm}$ are given by

$$Q_{\pm}^2 = (n+n'+1) \pm \sqrt{(2n+1)(2n'+1)},$$

where the probability $P_{nn'}$ exhibits characteristic classical singularities. The classical transition probability (2) satisfies detailed balance. The transition probability for elastic collision ($n=n'$) is

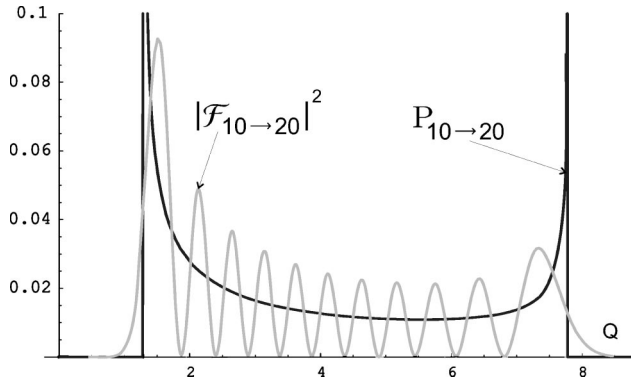


FIG. 1. Classical and quantal transition probabilities for the $(n=10) \rightarrow (n'=20)$ transition in the harmonic oscillator vs momentum transfer Q .

$$P_{nn'}(Q) = \frac{1}{\pi Q} [2(2n+1) - Q^2]^{-1/2}. \quad (3)$$

The advantage of using the classical transition probability is illustrated by the following example. Consider the $10 \rightarrow 20$ transition. The quantal expression deduced from Eq. (1),

$$\begin{aligned} \mathcal{F}_{10 \rightarrow 20}(Q) = & \frac{e^{-Q^2/2} Q^{10}}{5225472000 \sqrt{323323}} (-670442572800 \\ & + 609493248000 Q^2 - 228559968000 Q^4 \\ & + 46884096000 Q^6 - 5860512000 Q^8 \\ & + 468840960 Q^{10} - 24418800 Q^{12} \\ & + 820800 Q^{14} - 17100 Q^{16} + 200 Q^{18} - Q^{20}) \end{aligned}$$

is rather large, and is numerically inefficient due to the oscillations in the wave functions. The classical transition probability (2), however, has the simpler form

$$P_{10,20}(Q) = \frac{1}{\pi} \sqrt{-Q^4 + 62Q^2 - 100}$$

within the classically allowed range $31 - \sqrt{861} \leq Q^2 \leq 31 + \sqrt{861}$.

The classical $P_{nn'}$ and quantal $|\mathcal{F}_{nn'}|^2$ are compared in Fig. 1. The comparison exhibits excellent “background” agreement within the classically allowed region of Q , the characteristic classical singularities at Q_{\pm} , and the characteristic exponential quantal tails in the forbidden region. The number of quantal oscillations in $\mathcal{F}_{nn'}$ is given by $\min(n, n') + 1$ which occur within the extent $[(2n+1)(2n'+1)]^{1/2}$ centered on the median value $(n+n'+1)$ of the Q^2 range.

The classical transition probability for any momentum transfer (or the integrated form factor) is

$$\begin{aligned} P_{\text{if}} &= \int_{-\infty}^{\infty} P_{\text{if}}(Q) dQ \\ &= \frac{2}{\pi} \int_{Q_-}^{Q_+} [(Q^2 - Q_-^2)(Q_+^2 - Q^2)]^{-1/2} dQ, \end{aligned}$$

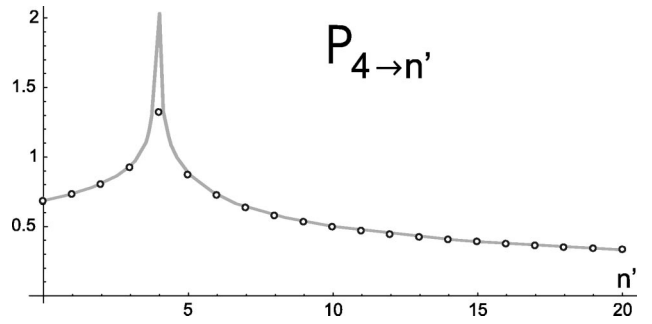


FIG. 2. Classical (solid line) and quantal (dots) transition probabilities for any momentum transfer q from the state $n=4$ to states $n'=0-20$.

which reduces to

$$P_{nn'} = \frac{2}{\pi Q_-} \left[F\left(\frac{\pi}{4} \middle| \frac{-s}{1-s}\right) + \sqrt{\frac{1-s}{s}} F\left(\arcsin \sqrt{\frac{s}{2}} \middle| \frac{1}{s}\right) \right]$$

where $s = 1 - Q_-^2/Q_+^2$

in terms of the incomplete elliptic function F .

Figure 2 shows that there is an excellent agreement between the quantal and classical transition probabilities for general $n \rightarrow n'$ transitions in the harmonic oscillator for any momentum transfer. The singularity at $n' = n$ arises from Eq. (3). The characteristic agreement is displayed in Fig. 2.

III. PHASE-SPACE EXPRESSION FOR THE FORM FACTOR

The quantal amplitude

$$\mathcal{F}_{\text{if}}(\mathbf{q}) = \langle \Psi_f(\mathbf{r}) | e^{i\mathbf{q} \cdot \mathbf{r}/\hbar} | \Psi_i(\mathbf{r}) \rangle_{\mathbf{r}} = \langle \Phi_f(\mathbf{p} + \mathbf{q}) | \Phi_f(\mathbf{p}) \rangle_{\mathbf{p}} \quad (4)$$

is expressed as the above integrations over either configuration space or over momentum space, where the momentum wave functions are defined as

$$\Phi(\mathbf{p}) = (2\pi\hbar)^{-3/2} \int \Psi(\mathbf{r}) \exp(-i\mathbf{q} \cdot \mathbf{r}/\hbar) d\mathbf{r}.$$

The transition probability

$$P_{\text{if}}(\mathbf{q}) = |\langle \Psi_f(\mathbf{r}) | e^{i\mathbf{q} \cdot \mathbf{r}/\hbar} | \Psi_i(\mathbf{r}) \rangle|^2 \quad (5)$$

can therefore be expressed as

$$\begin{aligned} & \langle \Psi_f(\mathbf{r}) | e^{i\mathbf{q} \cdot \mathbf{r}/\hbar} | \Psi_i(\mathbf{r}) \rangle_{\mathbf{r}} \langle \Phi_f(\mathbf{p} + \mathbf{q}) | \Phi_f(\mathbf{p}) \rangle_{\mathbf{p}} \\ &= \int d\mathbf{r} d\mathbf{p} [\Psi_f^*(\mathbf{r}) e^{i(\mathbf{p} + \mathbf{q}) \cdot \mathbf{r}/\hbar} \Phi_f(\mathbf{p} + \mathbf{q})] \\ & \quad \times [\Psi_i(\mathbf{r}) e^{-i\mathbf{p} \cdot \mathbf{r}/\hbar} \Phi_i^*(\mathbf{p})]. \end{aligned}$$

The quantal phase-space distribution may be defined by

$$\rho(\mathbf{r}, \mathbf{p}) = (2\pi\hbar)^{-3/2} \Psi(\mathbf{r}) e^{-i\mathbf{p} \cdot \mathbf{r}/\hbar} \Phi^*(\mathbf{p})$$

since the probability densities $\rho(\mathbf{r})$ in configuration space and $\rho(\mathbf{p})$ in momentum space (obtained by integrating the

quantal phase-space distribution over momentum or configuration space) yield $\rho(\mathbf{r}) = \int \rho(\mathbf{r}, \mathbf{p}) d\mathbf{p} = |\Psi(\mathbf{r})|^2$ and $\rho(\mathbf{p}) = |\Phi(\mathbf{p})|^2$, respectively. This distribution is the standard ordered version [10] of the Wigner distribution [11].

The transition probability is therefore

$$P_{if}(\mathbf{q}) = (2\pi\hbar)^3 \int d\mathbf{r} d\mathbf{p} \rho_i(\mathbf{r}, \mathbf{p}) \rho_f^*(\mathbf{r}, \mathbf{p} + \mathbf{q}). \quad (6)$$

This expression for the transition probability is now in a form appropriate for classical correspondence, obtained by replacing the quantal densities $\rho_{i,f}$ (even though $\rho_{i,f}$ have no direct physical interpretation) by the classical phase-space distributions $\rho^c(\mathbf{r}, \mathbf{p})$. Thus

$$P_{if}(\mathbf{q}) = (2\pi\hbar)^3 \int d\mathbf{r} d\mathbf{p} \rho_i^c(\mathbf{r}, \mathbf{p}) \rho_f^c(\mathbf{r}, \mathbf{p} + \mathbf{q}) \quad (7)$$

is the basic expression for the classical probability for impulsive transitions. The number of initial states in the phase-space element $d\mathbf{r} d\mathbf{p}$ is $\rho_i d\mathbf{r} d\mathbf{p}$, and $(2\pi\hbar)^3 \rho_f$ is the probability that the final state is in the same phase-space element.

Two fundamental properties, corresponding to similar properties of the quantal result (5), can be readily proven for the classical transition probability (7). The classical distributions satisfy

$$\rho(\mathbf{r}, \mathbf{p}) = \sum_n \rho_n(\mathbf{r}, \mathbf{p}) = (2\pi\hbar)^{-3},$$

which means that the total number states in the phase volume element is $d\mathbf{r} d\mathbf{p} / (2\pi\hbar)^3$, the number of elementary phase-space cells. The probability of transition from initial state i to all states f is then

$$\sum_f P_{if}(\mathbf{q}) = \int \rho_i(\mathbf{r}, \mathbf{p}) d\mathbf{r} d\mathbf{p} = g_i,$$

the statistical weight g_i of the initial state. The second property provides the transition probability for all momentum transfers \mathbf{q} . Integration of Eq. (7) over all possible values of the momentum transfer \mathbf{q} involves

$$\begin{aligned} \int \rho(\mathbf{r}, \mathbf{p} + \mathbf{q}) d\mathbf{q} &= \int \rho(\mathbf{r}, \mathbf{p}') d\mathbf{p}' \int \delta(\mathbf{p} + \mathbf{q} - \mathbf{p}') d\mathbf{q} \\ &= \rho(\mathbf{r}), \end{aligned}$$

where $\rho(\mathbf{r})$ is the classical distribution in configuration space. Then

$$\int P_{if}(\mathbf{q}) d\mathbf{q} = (2\pi\hbar)^3 \int \rho_i(\mathbf{r}) \rho_f(\mathbf{r}) d\mathbf{r}. \quad (8)$$

This classical property is again in correspondence with the quantal result

$$\int |\mathcal{F}_{if}(\mathbf{q})|^2 d\mathbf{q} = (2\pi\hbar)^3 \int |\Psi_i(\mathbf{r})|^2 |\Psi_f(\mathbf{r})|^2 d\mathbf{r}, \quad (9)$$

which can be derived from Eq. (4).

In the action-angle representation for bound states, the classical distribution is

$$\rho_n(\underline{J}, \underline{w}) d\underline{J} d\underline{w} = \delta(\underline{J}/h - \underline{n}) d\underline{J} d\underline{w} / (2\pi\hbar)^D$$

for a general D -dimensional system with a set of action-angle variables $(\underline{J}, \underline{w})$ in a state specified by the set of quantum numbers \underline{n} . The classical probability for $\underline{n} \rightarrow \underline{n}'$ transitions is therefore

$$\begin{aligned} P_{if}(\mathbf{q}) &= (2\pi\hbar)^{-D} \int \int \delta(\underline{J}/h - \underline{n}) \delta(\underline{J}'/h - \underline{n}') \\ &\quad \times \delta(\mathbf{p} + \mathbf{q} - \mathbf{p}') \delta(\mathbf{r} - \mathbf{r}') d\underline{J} d\underline{w} d\underline{J}' d\underline{w}', \quad (10) \end{aligned}$$

which provides a more general classical correspondence with the quantal expression (6), rewritten as

$$\begin{aligned} P_{if}(\mathbf{q}) &= (2\pi\hbar)^3 \int \int d\mathbf{r} d\mathbf{p} d\mathbf{r}' d\mathbf{p}' \rho_i(\mathbf{r}, \mathbf{p}) \rho_f(\mathbf{r}', \mathbf{p}') \\ &\quad \times \delta(\mathbf{r} - \mathbf{r}') \delta(\mathbf{p} + \mathbf{q} - \mathbf{p}'). \end{aligned}$$

These expressions emphasize the impulsive nature of the momentum transferred.

IV. FORM FACTOR FOR THE HYDROGENIC ATOM

A. Form factor for $nl \rightarrow n'l'$ transitions

The classical distribution for an atom with given energy E and angular momentum L , in (\mathbf{r}, \mathbf{p}) phase space is (Appendix A)

$$\begin{aligned} \rho(E, L; \mathbf{r}, \mathbf{p}) dE dL d\mathbf{r} d\mathbf{p} \\ = dE \delta(H - E_{nl}) dL \delta(|\mathbf{L}| - L) \frac{d\mathbf{r} d\mathbf{p}}{(2\pi\hbar)^3}, \quad (11) \end{aligned}$$

where both the Hamiltonian $H(\mathbf{r}, \mathbf{p}) = p^2/2m + V(r)$ and angular momentum $|\mathbf{L}(\mathbf{r}, \mathbf{p})| = rp \sin \theta_{rp}$ are constants of motion. The classical transition probability for the case of a central field one-electron atom, between the states, or bands of states centered at (E, L) and (E', L') , due to momentum transfer \mathbf{q} , is then

$$\begin{aligned} P(E, L; E', L'; \mathbf{q}) dE dL dE' dL' \\ = dE dL dE' dL' \int \frac{d\mathbf{r} d\mathbf{p}}{(2\pi\hbar)^3} \delta(H(\mathbf{r}, \mathbf{p}) - E) \\ \times \delta(|\mathbf{L}(\mathbf{r}, \mathbf{p})| - L) \delta(H(\mathbf{r}, \mathbf{p} + \mathbf{q}) - E) \\ \times \delta(|\mathbf{L}(\mathbf{r}, \mathbf{p} + \mathbf{q})| - L'). \quad (12) \end{aligned}$$

The quantity $P(\Gamma; \Gamma'; \mathbf{q})$ is the transition probability density (per unit intervals $d\Gamma d\Gamma'$). When E, E', L , or L' are quantized, the transition probability between corresponding states are obtained by the formal replacements $dE \rightarrow h\nu_{nl}$ and $dL \rightarrow \hbar$ on the right-hand side of Eq. (12). The transition probability between bound states with given quantum numbers (n, l) and (n', l') is then

$$P_{nl,n'l'}(\mathbf{q}) = h\nu_{nl} h\nu_{n'l'} \hbar^2 \times P(E_{nl}, (l+1/2)\hbar; E_{n'l'}, (l'+1/2)\hbar), \quad (13)$$

where $\nu_{nl} = \tau_{nl}^{-1}$ is the radial frequency of the classical orbit.

Since the densities used in Eq. (13) are already normalized to $(2l+1)$ particles in all of the phase space (see Appendix A), Eq. (13) represents the basic definition of the classical form factor, in direct correspondence with the (symmetrical) quantal form factor

$$F_{nl,n'l'}(\mathbf{q}) = \sum_m \sum_{m'} |\langle nlm | e^{i\mathbf{q}\cdot\mathbf{r}/\hbar} | n'l'm' \rangle|^2. \quad (14)$$

The physical significance of the basic expression (7) is that the initial and final states correspond to definite regions in phase space populated according to the microcanonical distributions (11). Transitions can only occur if these two regions overlap, and the amount of overlap is a measure of the transition probability. The classical form factor (13) which has been developed in detail in Appendix B, will be directly compared with the quantal result of Eq. (14), developed in Appendix C as a function of q for arbitrary $nl \rightarrow n'l'$ transitions.

The result of the classical calculation (13) (see Appendix B for details) is

$$P_{nl,n'l'}(\mathbf{q}) = \left[\frac{2(2l+1)(2l'+1)\hbar^3}{\tau_{nl}\tau_{n'l'}} \right] \times \int_{\mathcal{R}} \frac{dr/r^2}{r\dot{r}'} \left[\frac{G_{\text{if}}^+(r,q) + G_{\text{if}}^-(r,q)}{q} \right] \Theta(r,q), \quad (15)$$

where $\Theta(r,q)$ is the step function having value unity within $r < r^*$ (given in Appendix B), and zero otherwise, and the function

$$G_{\text{if}}^{\pm}(r,q) = \frac{1}{\sqrt{(q^2 - A_{\pm}^2)(B_{\pm}^2 - q^2)}} \quad (16)$$

must be real, so that q must be within the classically accessible range \mathcal{R} given by

$$A_{\pm}^2 = m^2(\dot{r} \pm \dot{r}')^2 + (L - L')^2 / r^2 \leq q^2 \leq B_{\pm}^2 = m^2(\dot{r} \pm \dot{r}')^2 + (L + L')^2 / r^2.$$

The radial velocity \dot{r} (\dot{r}') is a function only of r for a given nl (or $n'l'$) state. For a given momentum transfer q , the r integration proceeds over the radial ranges within which the square roots in Eq. (16) are real. This situation is illustrated in Fig. 3 for the $(4,3) \rightarrow (8,2)$ transition in the hydrogen

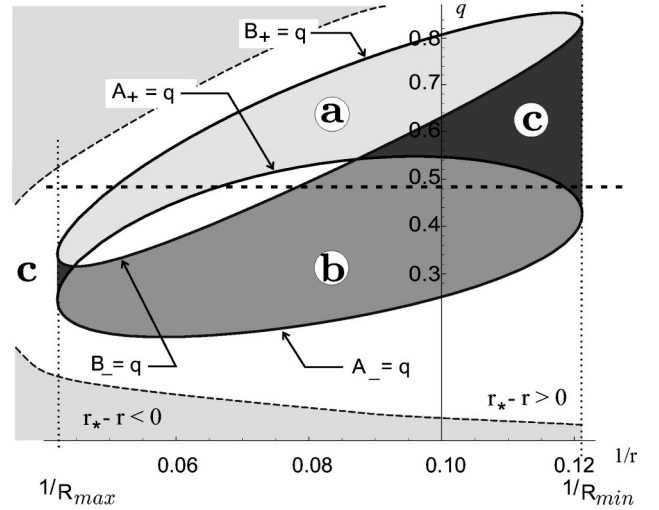


FIG. 3. Integration region for a typical $(4,3) \rightarrow (8,2)$ transition.

atom. The dotted curve is the boundary ($r_* - r = 0$) of the region within which the function Θ is unity, and which encompasses the physical accessible region $A_- \leq q \leq B_+$. When q is small (below the A_- curve) or large (above the B_+ curve), G_{if} has complex values and the transition probability is necessarily zero. In the shaded regions only G_{if}^+ (a) or G_{if}^- (b) or both G_{if}^{\pm} (c) can contribute to the integral for a given q . The range \mathcal{R} of radial integration always lies within the region specified by $A_+ = A_- = \text{real}$ and $B_+ = B_- = \text{real}$. The boundaries of this region are then given by $R_{\text{min}} = \max(R_i^-, R_f^-)$ and $R_{\text{max}} = \min(R_i^+, R_f^+)$, where R^- and R^+ are the pericenter and the apocenter of the Kepler orbit. The three situations possible (details in Ref. [3]) for the overlap of the initial and final orbits are illustrated in Fig. 4 as L' of the final orbit is increased. Region I gives the maximum overlap when region $\mathcal{R} = (R_i^-, R_i^+)$ is specified only by the initial state. In Region II the overlap is partial, because the lower limit of \mathcal{R} is given by the pericenter of the final orbit R_f^- . In Region III the pericenter R_f^- has moved outside R_i^+ , so that there is no overlap, the transition is classically forbidden.

The quantal transition probability for bound-bound transitions, for hydrogenic atoms, is a rational function in the momentum transfer q . The proof of this statement and the algorithm for quantal calculations are presented in Appendix C. The form factor for the $(4,3) \rightarrow (8,2)$ transition, as a function of q , is

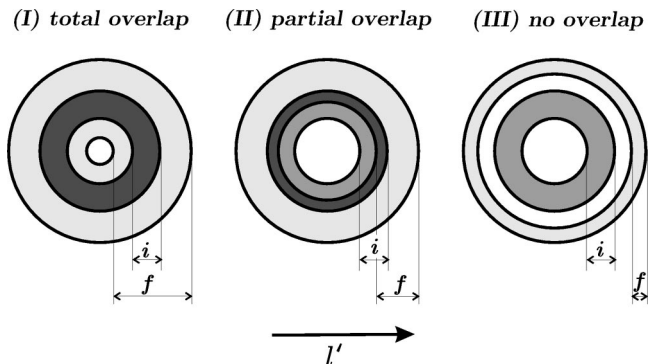


FIG. 4. Overlap situations for fixed initial n, l , and n' and varying l' .

$$\begin{aligned}
P_{4,3 \rightarrow 8,2}(q) = & \frac{34359738368q^2}{(9+64q^2)^{24}} (1977006755367 - 84352288228992q^2 - 52980973020131328q^4 + 914957411105636352q^6 \\
& + 557017745580707807232q^8 + 49144600326376878243840q^{10} + 1304678925402985186983936q^{12} \\
& - 12446991865892540818391040q^{14} + 839683843672479677596827648q^{16} \\
& + 5269768456130999660417384448q^{18} + 226149481324737121139390676992q^{20} \\
& - 3490013454414646748315148877824q^{22} + 22442701774022980630594896003072q^{24} \\
& - 63431755657397448352885433696256q^{26} + 66458636923717615551358326276096q^{28}).
\end{aligned}$$

The results of calculations for the quantal and classical probabilities (form factors) are compared in Fig. 5. The four singularities in the classical transition probability, which indicates maxima in quantal results, correspond with those values of the momentum transfer for which the ($q = \text{const}$) line is tangent to one of the curves $A \pm = q$ or $B \pm = q$ in Fig. 3. One of these equations has then a double root in r , which eventually yields after integration a logarithmic singularity.

In Fig. 6 the quantum numbers n, l , and n' are fixed and the transition probability versus the momentum transfer q is plotted for various final angular momenta l' . As l' increases, the quantal and classical transition probabilities increase, and attain a maximum for some value of l' . This value is roughly given by $l' \approx n\sqrt{2}$, in agreement with the results derived in Ref. [3]. Further increasing l' produces a sharp decrease in the quantal transition probability. The classical transition probability is forbidden for $l' = 6$ and 7, since there is no overlap at all between the phase-space regions occupied by the initial and the final states, for any momentum transfer q . This situation corresponds to region III of Fig. 4. The quantal results for $l' = 6$ and 7 are therefore classically inaccessible.

When the final principal quantum number n' is varied, keeping n, l , and l' fixed, the shape of the transition probability versus momentum transfer is preserved and the magnitude rapidly decreases as n' increases. This observation, valid for both quantal and classical cases, is demonstrated in Fig. 7 for a specific case. Because the transition probability (14) contains the factor $1/\tau' \sim 1/n'^3$, the classical form factor provides an explanation for this behavior.

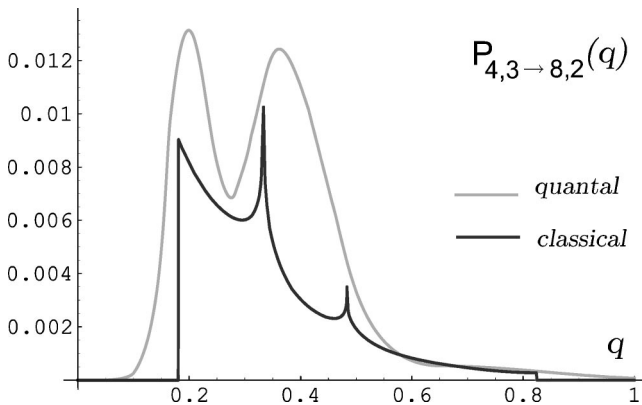


FIG. 5. Quantal and classical transition probabilities for the $(4,3) \rightarrow (8,2)$ transition.

When the final state is in the continuum with energy between E' and $E' + dE'$, result (15) is still valid provided $h\nu_{n'l'}$ is replaced by dE' . The probability for a bound-free transition is then

$$\begin{aligned}
P_{nl,l'}(E'; \mathbf{q}) dE' = & \left[\frac{(2l+1)(2l'+1)\hbar^2 dE'}{\pi \tau_{nl}} \right] \\
& \times \int_{\mathcal{R}} \frac{dr/r^2}{\dot{r}_1 \dot{r}_2} \left[\frac{G_{\text{if}}^+(r, q) + G_{\text{if}}^-(r, q)}{q} \right].
\end{aligned}$$

B. Integrated $nl \rightarrow n'l'$ form factor

The integrated form factor or the transition probability for any momentum transfer is the integral of the q -dependent transition probability over the q space. The quantal calculation gives

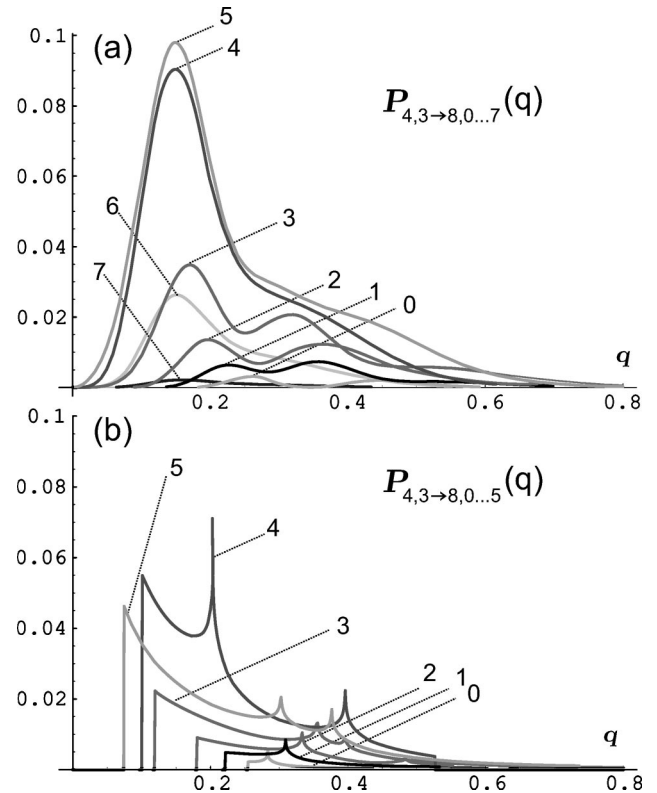


FIG. 6. Quantal (a) and classical (b) transition probabilities for the $(4,3) \rightarrow (8,l')$ transitions, with $l' = 0, \dots, 7$.

$$\int |F_{nl,n'l'}^q(\mathbf{q})|^2 d\mathbf{q} = (2\pi\hbar)^3 \int d\mathbf{q} \sum_m |\Psi_{nlm}(\mathbf{r})|^2 \sum_{m'} |\Psi_{n'l'm'}(\mathbf{r})|^2,$$

which, with $\Psi(\mathbf{r}) = (R_{nl}/r)Y_{lm}(\hat{r})$, reduces to

$$\int |F_{nl,n'l'}^q(\mathbf{q})|^2 d\mathbf{q} = 2\pi^2(2l+1)(2l'+1)\hbar^3 \int \rho_{nl}^q(r)\rho_{n'l'}^q(r)dr/r^2, \quad (17)$$

where $\rho^q(r)dr = R_{nl}^2(r)dr$ is the radial probability.

Integration of the corresponding classical transition probability (8) gives

$$\int P_{nl,n'l'}(\mathbf{q}) d\mathbf{q} = \frac{8\pi^2(2l+1)(2l'+1)\hbar^3}{\tau_1\tau_2} \int_{\mathcal{R}} \frac{(dr/r^2)}{\dot{r}_1\dot{r}_2}. \quad (18)$$

Upon integration, Eq. (18) yields

$$P_{nl,n'l'} = \frac{8}{n^3 n'^3} F(\arcsin\sqrt{s}|1/s) [(x_3-x_2)(x_4-x_1)]^{-1/2}$$

with $s = \frac{(x_3-x_2)(x_4-x_1)}{(x_3-x_1)(x_4-x_2)},$

where F is the incomplete elliptic function and x_i ($i = 1, 2, 3$, and 4) is the sorted set $(R_i^-, R_i^+, R_f^-, R_f^+)$. When there is no overlap between the initial and final states ($R_i^+ < R_f^-$) the transition is of course classically forbidden (situation III in Fig. 4). Comparison between the quantal and classical expressions reveals the definition of the classical radial probability: $\rho^c(r)dr = 2dt/\tau$, in agreement with the customary correspondence (deduced in Appendix A). The q integrated transition probabilities for fixed initial quantum numbers n and l and final n' as function of the final angular momentum l' are shown in Fig. 8. There is excellent agreement between the quantal and classical calculations before the first singularity in l' , which marks the transition from region I to region II in Fig. 4. For larger l' , the quantal transition probabilities oscillate about the classical transition probabilities. As proven in Ref. [3], there is a limiting value l'_* of l' after which the quantal transition probability exponentially decays while the classical form factor is zero. This situation corresponds with region III in Fig. 4, where the transition is classically forbidden. If this special value of l' cannot be accommodated, because $l'_* \geq n' - 1$, the transition is classically always permitted and the quantal transition probability has no exponential tail. This is the case of quasi elastic transitions (between the same principal quantum numbers), as presented in Fig. 9. For this case, the agreement

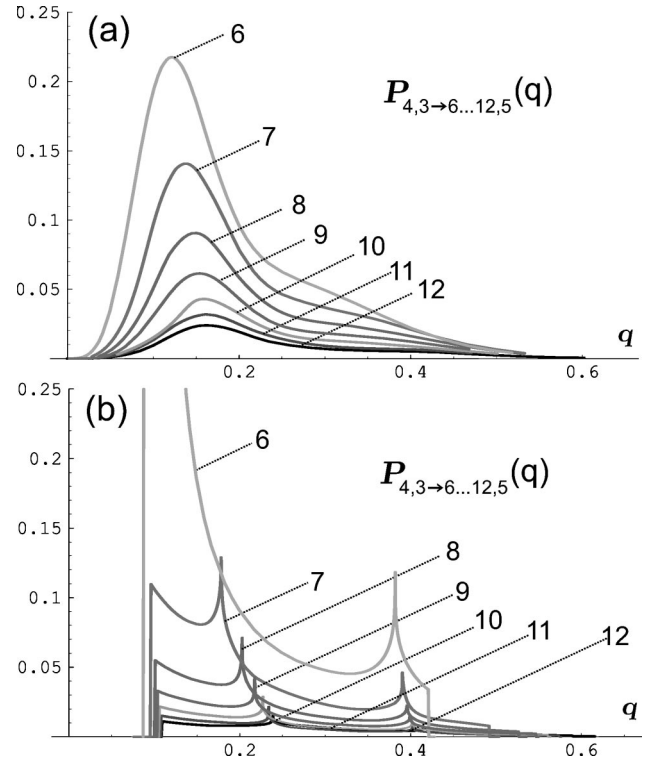


FIG. 7. Quantal (a) and classical (b) transition probabilities for the $(4,3) \rightarrow (n',5)$ transitions, with $n' = 6, \dots, 12$.

between quantal and classical calculations is excellent for any l' . The q -integrated form factors were discussed in Ref. [3].

C. Form factor for $nl \rightarrow n'$ transitions

Summation over the final angular momentum number l' provides the form factor

$$P_{nl,n'}(\mathbf{q}) = \sum_{l'=0}^{n'-1} \sum_{m,m'} |\langle nlm | e^{i\mathbf{q}\cdot\mathbf{r}/\hbar} | n'l'm' \rangle|^2. \quad (19)$$

The basic definition (7) gives the classical analog for this form factor:

$$P_{nl,n'}(\mathbf{q}) = (2\pi\hbar)^3 \int d\mathbf{r} d\mathbf{p} \rho_{nl}(\mathbf{r}, \mathbf{p}) \rho_{n'}(\mathbf{r}, \mathbf{p} + \mathbf{q}),$$

where the densities ρ_{nl} and l -averaged $\rho_{n'}$ are described in Appendix A. Using $V(r) = E - p^2/2m$, the final distribution is rewritten in the r independent form as

$$\rho_{n'}(\mathbf{r}, \mathbf{p} + \mathbf{q}) = (h\nu_{n'}) \delta[(\mathbf{p} + \mathbf{q})^2/2m - p^2/2m + E - E'] / (2\pi\hbar)^3.$$

where \mathbf{r} means “not \mathbf{r} .” The classical transition probability for impulsive $nl \rightarrow n'$ transitions is then

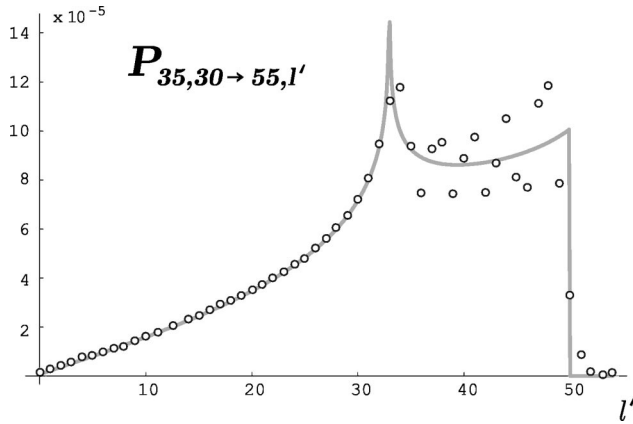


FIG. 8. Quantal (dots) and classical (solid line) transition probabilities for the (35,30) \rightarrow (55, l') transitions, with $l'=0, \dots, 54$.

$$P_{nl,n'}(\mathbf{q}) = \int d\mathbf{p} \rho_{nl}(\mathbf{p}) \rho_{n'}(\mathbf{p} + \mathbf{q}),$$

which is the classical overlap only of the momentum space distributions, rather than the full phase-space distributions, as in Eq. (12) for $nl \rightarrow n'l'$ transitions. Since

$$\int \delta(pq \cos \theta_{pq}/m + q^2/2m + E - E') d\hat{p} = 2\pi m/pq$$

for $p > p_0 = |2m(E' - E) - q^2|/2q$, and zero otherwise, this transition probability reduces to

$$P_{nl,n'}(q) = \frac{2\pi m}{q} (h\nu_{n'}) \int_{p_0}^{\infty} \rho_{nl}(\mathbf{p}) p dp,$$

which involves only the momentum distribution of the initial state. The same result is also obtained in Appendix B by

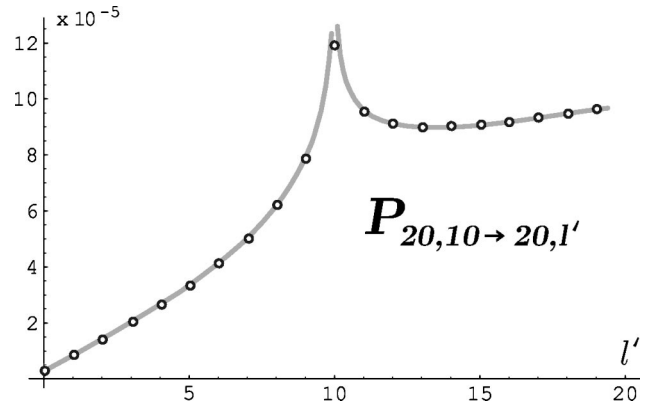


FIG. 9. Quantal (dots) and classical (solid line) transition probabilities for the (20,10) \rightarrow (20, l') transitions, with $l'=0, \dots, 19$.

(summing) integrating the original probability $P_{nl,n'l'}$ over all possible final angular momenta. The probability for $n, l \rightarrow n'$ transitions in hydrogen is

$$P_{nl,n'}(q) = \frac{2(2l+1)}{\pi q n'^3} \int_{p_{\min}}^{p_+} \frac{n}{p} (1+n^2 p^2)^{-2} \times \left[1 - \left(\frac{L(1+n^2 p^2)}{2n^2 p} \right)^2 \right]^{-1/2}, \quad (20)$$

where all quantities are in atomic units, and $L = l + 1/2$. The limits of integration are given by $p_{\min} = \max[p_0 = |q^2 + 1/n'^2 - 1/n^2|/2q, p_-]$, where $p_{\pm} = (1 \pm (1 - L^2/n^2)^{1/2})/L$ are the extreme values (at pericenter and apocenter) of the momentum of the electron on a given orbit. As a specific example, consider the 4,3 \rightarrow 8 transition. The quantal form factor is (cf. Appendix C)

$$P_{4,3 \rightarrow 8}(q) = \frac{34359738368 q^2}{5(9 + 64 q^2)^{17}} (9721215 + 4498478208 q^2 + 471603326976 q^4 + 6554684489728 q^6 - 451062079160320 q^8 + 6344423684177920 q^{10} - 12676750592966656 q^{12} - 12899470417068032 q^{14} + 535928355657089024 q^{16} + 450359962737049600 q^{18}).$$

The classical and quantal form factors, are compared in Fig. 10. The insets show the p integration range as a function of the momentum transfer q . Three special cases are presented: (a) excitation, (b) quasielastic transition, and (c) deexcitation. For q sufficiently small that $p_0 > p_+$, the transition is classically forbidden [cases (a) and (c)]. As q increases, the integration limits of Eq. (20) are (p_0, p_+) . The increase of P in cases (a) and (c) is due to the effect of increasing range of integration overwhelming the background q^{-1} decrease. With a further increase in q , the inte-

gration limits change to (p_-, p_+) which are independent of q . Here P decreases purely as q^{-1} , as in (a) and (b). For larger q , the more rapid decrease in P results from a q^{-1} variation combined with the effect of a decreasing range of integration, as exhibited for all cases. The transition is again classically forbidden, for all cases, in the limit of large q when $p_0 > p_+$. These three overlap situations described above are illustrated in Fig. 11. For deexcitation ($E' < E$), p_0 has always one minimum value $p_0^* = [2m(E - E')]^{1/2}$. When $p_0^* > p_-$, then the pattern of case (c), with momentum

limits (p_0, p_-), is established. This occurs for de-excitation to levels $n' < n_+(n, L) = (L/\sqrt{2})[1 - (1 - L^2/n^2)^{1/2}]^{-1/2}$. De-excitation to levels $n' > n_+$ is characterized by the pattern of case (c). When $p_0^* > p_+$, transitions are classically forbidden. This occurs for de-excitation to final states, $n' < n_-(n, L) = (L/\sqrt{2})[1 + (1 - L^2/n^2)^{1/2}]^{-1/2}$, whose orbits are fully within the orbit of the initial (n, L) state. The n_- limit therefore delineates the classically allowed from classically forbidden de-excitation transitions. The n_{\pm} demarcations are illustrated in Fig. 11. For excitation, p_0 can be zero at $q^* = [2m(E' - E)]^{1/2}$, so that there is always a range of transition momenta q for which $p_0 < p_-$ i.e. $n' > n_+(n, L)$. Excitation is therefore always characterized by the pattern of case (a). The quantal-classical agreement for $nl \rightarrow n'$ transitions is overall very good.

D. Form factor for $n \rightarrow n'$ transitions

The classical probability of transition between states specified only by their principal quantum numbers as function of the dimensionless parameter $Q = qa_0/Z\hbar$ (as derived in Appendix B) is

$$P_{n,n'}(Q) = \frac{2^9}{3\pi(nn')^3} Q^5 \left[Q^4 + 2 \left(\frac{1}{n^2} + \frac{1}{n'^2} \right) Q^2 + \left(\frac{1}{n^2} - \frac{1}{n'^2} \right)^2 \right]^{-3},$$

which is the classical correspondence of

$$P_{n,n'}(\mathbf{q}) = \sum_{l=0}^{n-1} \sum_{l'=0}^{n'-1} \sum_{m,m'} |\langle nlm | e^{i\mathbf{q} \cdot \mathbf{r}/\hbar} | n'l'm' \rangle|^2. \quad (21)$$

This quantal form factor (as derived in Appendix C) is again a rational function in the momentum transfer q since is a summation of $P_{nl n'l'}$ form factors. The classical result is in agreement with the result deduced by Vriens [9] from comparison of binary-encounter and Bethe treatments of electron-atom collisions, and by Borodin [12] from the microcanonical phase space distribution $\delta(H - E)$.

Exact quantal and classical form factors for $6 \rightarrow 40$ transitions are compared in Fig. 12. The expression for the quantal form factor for this specific transition

$$\begin{aligned} P_{6 \rightarrow 40}(q) = & \frac{382205952 \cdot 10^7 q^2 (289 + 14400 q^2)^{32}}{(529 + 14400 q^2)^{48}} (609748651778452988718867471792636791 \\ & + 1411176845994965835001817764524075792 \times 10^2 q^2 - 184318171941496097624317093441846656 \\ & \times 10^5 q^4 + 93670997716818370857325330958800896 \times 10^7 q^6 - 2400432080403014981637748114489344 \\ & \times 10^{10} q^8 + 34865881226093843259112916256817152 \times 10^{10} q^{10} - 2927694744198493018588901567102976 \\ & \times 10^{12} q^{12} + 14387567274612996874680196399104 \times 10^{15} q^{14} - 395454399288571654223098281984 \\ & \times 10^{17} q^{16} + 5960746343048968862171136 \times 10^{22} q^{18} - 396176923859529631650545664 \times 10^{20} q^{20} \\ & + 1656184316737309252780032 \times 10^{22} q^{22}) \end{aligned}$$

is an application of the general expression for transitions $6 \rightarrow n'$ presented in Table I. These results are derived in Appendix B (classical form factor) and Appendix C (quantal form factor). Due to the correspondence principle, there is excellent agreement between the quantal and more compact classical expressions $n' \gg n \gg 1$. The agreement is also expected because the characteristic classical singularities in the form factor are “smoothed” after the l, l', m , and m' summations.

V. SUMMARY AND CONCLUSIONS

Based on the phase-space description of an atomic system, classical expressions for the inelastic form factor have been derived. The formulas obtained are the exact classical correspondences of the quantal form factors. The classical methods quite succinctly reveals important aspects which remain hidden in the quantum treatment. An efficient algorithm for calculation of quantal form factors as analytical

functions of momentum transfer q , for arbitrary initial and final states, has also been developed.

For $nl \rightarrow n'l'$ transitions, the classical method provides both the qualitative behavior of the quantum results and its physical interpretation. The classical-quantal agreement is particularly noteworthy for the integrated form factors (cf. Figs. 8 and 9) for inelastic and quasielastic transitions. This is because both classical and quantal form factors depend only on the overlap of the initial and final distributions in configuration space [cf. Eqs. (17) and (18)], so that the classical singularities apparent in Fig. 5 are averaged to produce the smooth results in Figs. 8 and 9.

The increasing accuracy obtained upon l' integration is due to the absence of the multiple delineation of the phase space associated with $nl \rightarrow n'l'$ transitions (see Fig. 3). Again the classical picture not only provides the physical explanation for the quantal behavior when the momentum transfer q and quantum numbers are varied, but also identifies the patterns associated with each type (excitation, quasi-

elastic, and de-excitation) of transition (cf. Fig. 10). The agreement between classical and quantal integrated form factors is again excellent. In the limit of summing over all final states, the total transition probability is $\sum_f P_{if}(\mathbf{q}) = g_i$, the same result for both quantal and classical cases, which ensures full agreement in this limit.

On integrating over angular momentum quantum number l for $n \rightarrow n'$ transitions, the agreement is excellent for all q even for small quantum numbers. This is due to the fact that the phase-space region common to the both initial and final states (a sphere in configuration space with of radius r_*) is densely and continuously populated.

The classical form factors represent an attractive approach for classical collision theory. The form factor is a collision kernel to be convoluted according to the dynamics of the external interaction causing the transition. Due to the oscillatory nature of the wave functions, quantal calculations for processes involving highly excited states are still computationally expensive (in terms of precision, memory, and/or

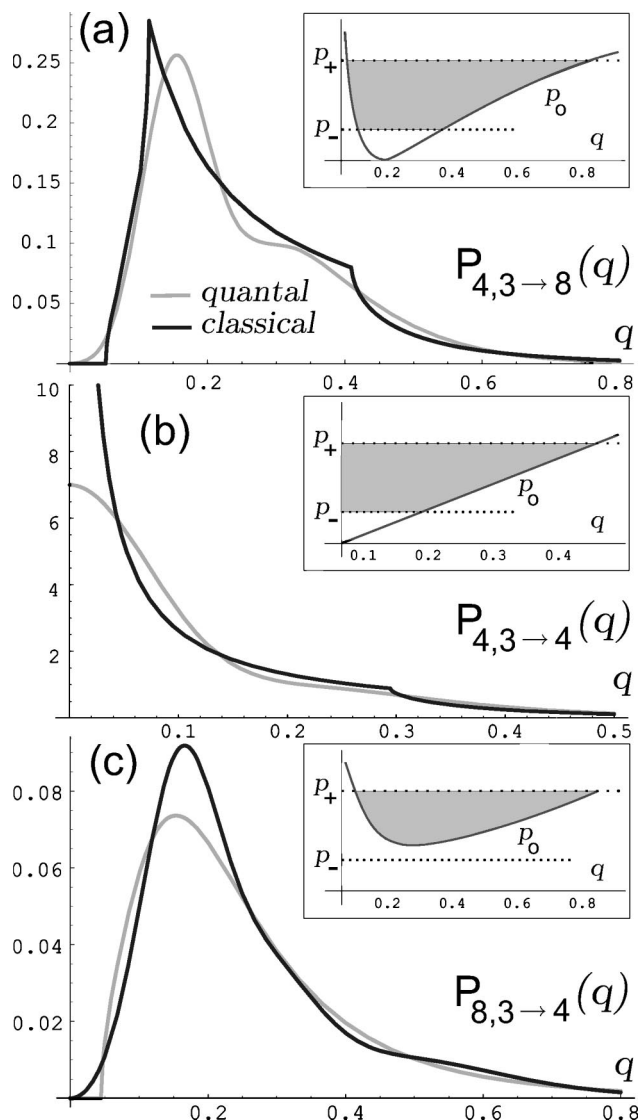


FIG. 10. Quantal and classical transition probabilities for (a) $(4,3) \rightarrow 8$, (b) $(4,3) \rightarrow 4$, and (c) $(8,3) \rightarrow 4$ transitions as a function of the momentum transfer. Insets: the gray area is the integration range.

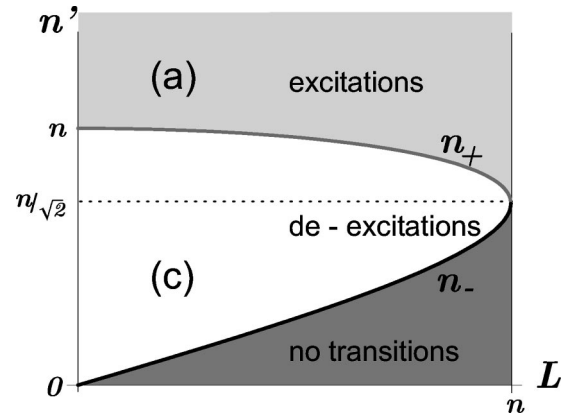


FIG. 11. The three overlap situations in momentum space: in region (a) there is a value of q for which $p_0 < p_-$; in region (c) $p_0 > p_-$ for any q , even though $p_0 < p_+$ for some q ; in shaded region transitions are classically forbidden, $p_0 > p_+$

time), while classical models are capable of exact results, according to the correspondence principles [4]. Although classical-quantal comparisons have been made to the one-dimensional harmonic oscillator and to hydrogenic systems, classical form factors can be useful for other atomic and molecular systems. The present method would also be valuable in determining the response of the three-dimensional Rydberg atom to a train of unidirectional short pulses of electromagnetic radiation [1]. The classical form factor methods would be also useful for excited-atom collisions [13].

ACKNOWLEDGMENTS

This work was supported by AFOSR Grant No. 49620-96-1-0142 and NSF Grant No. 98-02622. One of us (D.V.) thanks Motorola for generous support.

APPENDIX A: MICROCANONICAL DISTRIBUTIONS

The basic classical probability density for a particle moving in a symmetrical potential $V(r)$ is given by the microcanonical distribution

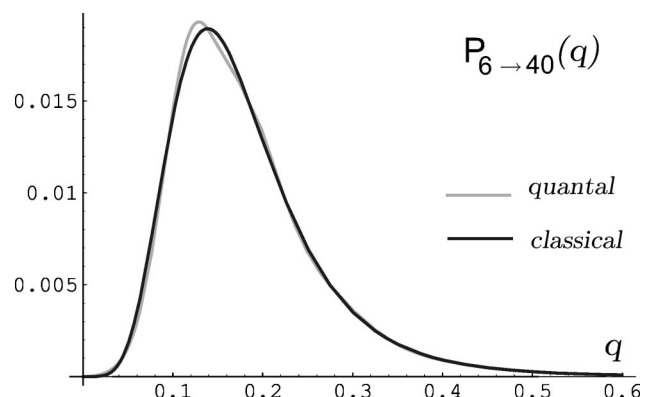


FIG. 12. Quantal and classical transition probabilities for the $6 \rightarrow 40$ transition as a function of the momentum transfer.

TABLE I. Quantal form factor [Eq. (21) from text] for $n' \rightarrow n$ transitions.

n'	$P_{nn'}(q) = \frac{2^8 n^7 q^2 [(n/n' - 1)^2 + q^2 n^2]^{(n-n'-2)}}{3 n'^3 [(n/n' + 1)^2 + q^2 n^2]^{(n+n'+2)}} \times$
1	$-1 + n^2 + 3 n^2 q^2$
2	$3 q^6 n^6 + 5 q^4 n^4 + q^2 n^2 + 9 n^2/4 - 23 n^4/16 + 15 n^6/64 - 9 n^4 q^2/2 + 65 n^6 q^2/16 - 11 n^6 q^4/4 - 1$
3	$3 q^{10} n^{10} + 11 q^8 n^8 + 14 q^6 n^6 + 6 q^4 n^4 - q^2 n^2 + 71 n^2/27 - 62 n^4/27 + 1790 n^6/2187 - 2431 n^8/19683$ $+ 377 n^{10}/59049 - 4 n^4 q^2/9 + 290 n^6 q^2/81 - 1460 n^8 q^2/729 + 1943 n^{10} q^2/6561 - 122 n^6 q^4/9 + 310 n^8 q^4/27$ $- 442 n^{10} q^4/243 - 412 n^8 q^6/27 + 518 n^{10} q^6/81 - 43 n^{10} q^8/9 - 1$
4	$3 q^{14} n^{14} + 17 q^{12} n^{12} + 39 q^{10} n^{10} + 45 q^8 n^8 + 25 q^6 n^6 + 3 q^4 n^4 - 3 q^2 n^2 + 45 n^2/16 - 2131 n^4/768 + 5093 n^6/4096$ $- 167011 n^8/589824 + 35231 n^{10}/1048576 - 32899 n^{12}/16777216 + 106183 n^{14}/2415919104 + 41 n^4 q^2/8 - 269 n^6 q^2/256$ $- 3475 n^8 q^2/3072 + 107449 n^{10} q^2/196608 - 128581 n^{12} q^2/1572864 + 201047 n^{14} q^2/50331648 - 217 n^6 q^4/16$ $+ 2691 n^8 q^4/128 - 59239 n^{10} q^4/6144 + 333157 n^{12} q^4/196608 - 290087 n^{14} q^4/3145728 - 197 n^8 q^6/4 + 16273 n^{10} q^6/384$ $- 34543 n^{12} q^6/3072 + 188555 n^{14} q^6/196608 - 917 n^{10} q^8/16 + 8027 n^{12} q^8/256 - 16035 n^{14} q^8/4096 - 239 n^{12} q^{10}/8$ $+ 2119 n^{14} q^{10}/256 - 95 n^{14} q^{12}/16 - 1$
5	$3 q^{18} n^{18} + 23 q^{16} n^{16} + 76 q^{14} n^{14} + 140 q^{12} n^{12} + 154 q^{10} n^{10} + 98 q^8 n^8 + 28 q^6 n^6 - 4 q^4 n^4 - 5 q^2 n^2 + 73 n^2/25$ $- 28828 n^4/9375 + 24084 n^6/15625 - 1475182 n^8/3515625 + 29028838 n^{10}/439453125 - 4495228 n^{12}/732421875$ $+ 90535316 n^{14}/274658203125 - 12906833 n^{16}/1373291015625 + 1251587 n^{18}/11444091796875 + 56 n^4 q^2/5$ $- 13876 n^6 q^2/1875 + 75224 n^8 q^2/46875 + 319042 n^{10} q^2/3515625 - 7425752 n^{12} q^2/87890625 + 9110956 n^{14} q^2/732421875$ $- 8239208 n^{16} q^2/10986328125 + 4510567 n^{18} q^2/274658203125 - 4 n^6 q^4/5 + 6836 n^8 q^4/375 - 673004 n^{10} q^4/46875$ $+ 3108484 n^{12} q^4/703125 - 18475444 n^{14} q^4/29296875 + 2024596 n^{16} q^4/48828125 - 54614636 n^{18} q^4/54931640625$ $- 1912 n^8 q^6/25 + 178396 n^{10} q^6/1875 - 672976 n^{12} q^6/15625 + 10191692 n^{14} q^6/1171875 - 22581416 n^{16} q^6/29296875$ $+ 18069764 n^{18} q^6/732421875 - 914 n^{10} q^8/5 + 59212 n^{12} q^8/375 - 2347228 n^{14} q^8/46875 + 1541158 n^{16} q^8/234375$ $- 2802002 n^{18} q^8/9765625 - 5272 n^{12} q^{10}/25 + 1233332 n^{14} q^{10}/9375 - 1272296 n^{16} q^{10}/46875 + 2099902 n^{18} q^{10}/1171875$ $- 676 n^{14} q^{12}/5 + 6996 n^{16} q^{12}/125 - 17868 n^{18} q^{12}/3125 - 232 n^{16} q^{14}/5 + 6076 n^{18} q^{14}/625 - 167 n^{18} q^{16}/25 - 1$
6	$3 q^{22} n^{22} + 29 q^{20} n^{20} + 125 q^{18} n^{18} + 315 q^{16} n^{16} + 510 q^{14} n^{14} + 546 q^{12} n^{12} + 378 q^{10} n^{10} + 150 q^8 n^8 - 70 q^6 n^6 + 15 q^4 n^4$ $- 15 q^2 n^2 + 323 n^2/108 - 1417 n^4/432 + 1230149 n^6/699840 - 6667507 n^8/12597120 + 43800179 n^{10}/453496320$ $- 33636707 n^{12}/3023308800 + 805306763 n^{14}/979552051200 - 8183128999 n^{16}/211583243059200$ $+ 8488861159 n^{18}/7616996750131200 - 4894595653 n^{20}/274211883004723200 + 398746151 n^{22}/3290542596056678400$ $+ 35 n^4 q^2/2 - 18907 n^6 q^2/1296 + 157637 n^8 q^2/29160 - 781087 n^{10} q^2/839808 + 1290871 n^{12} q^2/25194240$ $- 167865689 n^{14} q^2/27209779200 - 57381211 n^{16} q^2/48977602560 + 5399280829 n^{18} q^2/70527747686400$ $- 117424517 n^{20} q^2/50779978334208 + 2465858993 n^{22} q^2/91403961001574400 + 905 n^6 q^4/36 + 7 n^8 q^4/108$ $- 43949 n^{10} q^4/3888 + 4792471 n^{12} q^4/839808 - 188652173 n^{14} q^4/151165440 + 4792471 n^{12} q^4/839808$ $- 188652173 n^{14} q^4/151165440 + 77931593 n^{16} q^4/544195584 - 32278661 n^{18} q^4/3627970560$ $+ 264468259 n^{20} q^4/940369969152 - 594305017 n^{22} q^4/169266594447360 + 43385 n^{10} q^6/324 - 1458407 n^{12} q^6/17496$ $- 60952999 n^{14} q^6/2519424 - 82299863 n^{16} q^6/22674816 + 470998955 n^{18} q^6/1632586752$ $- 111918155 n^{20} q^6/9795520512 + 166167173 n^{22} q^6/940369969152 - 6335 n^{10} q^8/18 + 258155 n^{12} q^8/648$ $- 4222535 n^{14} q^8/23328 + 11088691 n^{16} q^8/279936 - 43657751 n^{18} q^8/10077696 + 1017419 n^{20} q^8/4478976$ $- 58621799 n^{22} q^8/13060694016 - 6167 n^{12} q^{10}/9 + 128209 n^{14} q^{10}/216 - 2015063 n^{16} q^{10}/9720 + 141006431 n^{18} q^{10}/4199040$ $- 61592369 n^{20} q^{10}/25194240 + 13034627 n^{22} q^{10}/201553920 - 14035 n^{14} q^{12}/18 + 170017 n^{16} q^{12}/324$ $- 23723233 n^{18} q^{12}/174960 + 12337645 n^{20} q^{12}/839808 - 27182041 n^{22} q^{12}/50388480 - 5030 n^{16} q^{14}/9 + 90701 n^{18} q^{14}/324$ $- 93505 n^{20} q^{14}/1944 + 737941 n^{22} q^{14}/279936 - 8995 n^{18} q^{16}/36 + 36175 n^{20} q^{16}/432$ $- 37405 n^{22} q^{16}/5184 - 3455 n^{20} q^{18}/54 + 14045 n^{22} q^{18}/1296 - 259 n^{22} q^{20}/36 - 1$

 $\rho(E, L, L_z; \mathbf{r}, \mathbf{p}) dE dL dL_z d\mathbf{r} d\mathbf{p}$

$$= \left\{ \delta(H - E) dE \delta(|\mathbf{L}| - L) dL \delta(\mathbf{L} \cdot \hat{\mathbf{z}} - L_z) dL_z \right\} \frac{d\mathbf{r} d\mathbf{p}}{(2\pi\hbar)^3}, \quad (\text{A1})$$

where the Hamiltonian H , angular momentum $|\mathbf{L}|$, and the projection of the angular momentum on z axis $\mathbf{L} \cdot \hat{\mathbf{z}}$ are conserved quantities, and specify the state of the system. Various other less restrictive [14] distributions are directly de-

duced from Eq. (A1) by dropping from Eq. (A1) those δ functions which correspond with the restrictions on the state of the system to be relaxed. For example, when the projection L_z of the angular momentum is arbitrary, the distribution is

$$\rho(E, L; \mathbf{r}, \mathbf{p}) dE dL d\mathbf{r} d\mathbf{p} = \left\{ \delta(H - E) dE \delta(|\mathbf{L}| - L) dL \right\} \frac{d\mathbf{r} d\mathbf{p}}{(2\pi\hbar)^3}, \quad (\text{A2})$$

and describes a population of $2L$ states in all of phase space. The physical interpretation is that Eq. (A2) is the number of states (phase-space cells) compatible with energy and angular momentum conservation. The $\{ \}$ factor is a fractional number of states in the interval $dE dL dL_z$ of about (E, L, L_z) .

If the system is described in terms of discrete quantum numbers, e.g., the motion is bounded within a finite spatial region, the classical distribution is defined in the action-angle representation by

$$\rho_{nlm} dJ d\omega = \delta(J_1/h - n) \delta(J_2/h - (l + 1/2)) \\ \times \delta(J_3/h - m) \frac{dJ d\omega}{(2\pi\hbar)^3}.$$

Upon action-angle variables (J, ω) integration, this distribution corresponds to a single particle in all of phase space. Also $\sum_{nlm} \rho_{nlm} = (2\pi\hbar)^{-3}$ is the number of particles in all states occupying the unit phase-space element. The phase-space distribution for state nl is

$$\rho_{nl} dJ d\omega = \delta(J_1/h - n) \delta[J_2/h - (l + 1/2)] \\ \times \frac{dJ_1 dJ_2 dJ_3 d\omega_1 d\omega_2 d\omega_3}{(2\pi\hbar)^3}.$$

Since $J_3 = J_2 \cos \hat{L} \cdot \hat{z}$, the J_3 integration gives $2J_2$, so that the above ρ_{nl} distribution corresponds to a population of $(2l + 1)$ states in all of phase space. The corresponding distribution in (\mathbf{r}, \mathbf{p}) phase space is then, by changing variables

$$\rho_{nl} d\mathbf{r} d\mathbf{p} = h^2 \left[\frac{\partial H(J_1, J_2)}{\partial J_1} \right] \left[\frac{\partial L(J_2)}{\partial J_2} \right] \delta(H(\mathbf{r}, \mathbf{p}) - E_{nl}) \\ \times \delta(|\mathbf{L}(\mathbf{r}, \mathbf{p})| - L) \frac{d\mathbf{r} d\mathbf{p}}{(2\pi\hbar)^3}.$$

Since $\partial H/\partial J_1 = \nu_{nl} = \tau_{nl}^{-1}$, the frequency (or inverse period) for radial bounded motion, then

$$\rho_{nl}(\mathbf{r}, \mathbf{p}) d\mathbf{r} d\mathbf{p} = \{h\nu_{nl} \delta(H - E_{nl}) \hbar \delta(|\mathbf{L}| - L)\} \frac{d\mathbf{r} d\mathbf{p}}{(2\pi\hbar)^3}. \quad (\text{A3})$$

This result can be obtained, formally, from Eq. (A2), by replacing dE and dL by $h\nu_{nl}$ and \hbar , respectively. The separation between highly excited neighboring energy levels n and $n \pm 1$ is $h\nu_{nl}$, the Bohr correspondence, and \hbar is the separation between neighboring angular momentum levels n, l and $n, l \pm 1$.

By noting that

$$\int_{-1}^1 \delta(rp \sin \theta - L) d(\cos \theta) = \frac{2L}{rp} (r^2 p^2 - L^2)^{-1/2},$$

$$p \geq L/r = p_0$$

and

$$\int_{p_{\min}}^{\infty} \delta(p^2/2m + V(r) - E_{nl}) \frac{p dp}{(r^2 p^2 - L^2)^{1/2}} \\ = \frac{m}{(r^2 p_+^2 - L^2)^{1/2}} = 1/(r\dot{r})$$

for $p_+^2 = 2m(E_{nl} - V(r)) \geq p_{\min}^2$, which ensures real radial speeds \dot{r} , then

$$\int \delta(H - E_{nl}) \delta(|\mathbf{L}| - L) d\mathbf{r} d\mathbf{p} = 8\pi^2 L \oint \frac{dr}{\dot{r}} = 8\pi^2 L / \nu_{nl}.$$

Distribution (A3) is thus confirmed as being normalized to $(2l + 1)$ states.

Since $d\mathbf{r} d\mathbf{p}/(2\pi\hbar)^3$ is the total number of bound and continuum states, with all quantum numbers, in the phase-space volume element $d\mathbf{r} d\mathbf{p} = dJ d\omega$, then the $\{ \}$ factor in (A3) represents the fractional number of states with specific quantum numbers.

For the particular case of Coulomb attraction the energy levels are degenerate. The phase-space distribution for an hydrogenic atom in the energy level E_n , corresponding with the principal quantum number n , is

$$\rho_n(\mathbf{r}, \mathbf{p}) d\mathbf{r} d\mathbf{p} = h\nu_n \delta(H - E_n) \frac{d\mathbf{r} d\mathbf{p}}{(2\pi\hbar)^3} \quad (\text{A4})$$

for bound states of degeneracy n^2 . The same expression holds for states in the continuum if $h\nu_n$ is replaced by dE .

The classical distribution $\rho_{nl}(\mathbf{r}) = \int \rho_{nl}(\mathbf{r}, \mathbf{p}) d\mathbf{p}$ in configuration space is

$$\rho_{nl}(r) r^2 dr d\hat{r} = \frac{g_l}{\tau_{nl}} \frac{2 dr}{\dot{r}} \frac{d\hat{r}}{4\pi}$$

where $g_l = 2l + 1$ is the statistical weight of the nl level. For Coulombic attraction, $V(r) = -Ze^2/r$, $\tau_n = 2\pi n^3$ a.u., and

$$4\pi \rho_{nl}(r) r^2 dr = R_{nl}(r) dr \\ = \frac{1}{\pi n^3} \left(\frac{2Z}{r_{\text{a.u.}}} - \frac{Z^2}{n^2} - \frac{(l + 1/2)^2}{r_{\text{a.u.}}^2} \right)^{-1/2} dr$$

for one nl state ($g_l = 1$).

Integration of Eq. (A2) over the configuration space yields the momentum space distribution $\rho(E, L; \mathbf{p}) = \int \rho(E, L; \mathbf{r}, \mathbf{p}) d\mathbf{r}$. Then

$$\rho(E, L; p) p^2 dp d\hat{p} \\ = \frac{g_l}{2\pi\hbar^2} \left[\sum_i \frac{2 p dp}{(p^2 - L^2/r_i^2)^{1/2}} \frac{1}{|V'(r_i)|} \right] \frac{d\hat{p}}{4\pi}, \quad (\text{A5})$$

where r_i are the roots of $p^2 = 2m[E - V(r)]$ for a given p and $V' = dV/dr$. The radial momentum distribution, $\rho_{nl} = \rho(E, L) h\nu_{nl} \hbar$, for bound hydrogenic states, reduces with $g_l = 1$ to

$$\rho_{nl}(p) 4\pi p^2 dp = \left(\frac{2Ze^2 dp}{\tau_n |E|^2} \right) (1+x^2)^{-2} \times \left(1 - \frac{2m|E|L^2}{(2mZe^2)^2} \frac{(x^2+1)^2}{x^2} \right)^{-1/2},$$

where $x = p/(2m|E|)^{1/2}$. Since $E = -Z^2(e^2/a_0)/2n^2$, then $x = p/p_n$ where $p_n = Zp_0/n$ is the characteristic momentum in the Rydberg orbit n , $p_0 = \hbar/a_0$ is the atomic unit for linear momentum, and a_0 the Bohr radius is the atomic unit for distance. With $L = (l+1/2)\hbar$, the hydrogenic momentum distribution is

$$\rho_{nl}(p) 4\pi p^2 dp = \frac{4}{\pi} n \frac{dP}{(1+n^2P^2)^2} \left\{ 1 - \left[\frac{l+1/2}{n} \right] \times \left(\frac{1+n^2P^2}{2nP} \right)^2 \right\}^{-1/2},$$

where $P = p/Zp_0$. This compares formally with the quantal results and is useful for the $nl \rightarrow n'$ classical form factor. Another formulation of classical momentum distributions was recently presented in Ref. [15].

APPENDIX B: CALCULATIONS OF CLASSICAL FORM FACTORS

The classical form factor for transitions between energy and angular momentum bands ($E, E+dE; L, L+dL$) is

$$P_{if}(\mathbf{q}) = P(E, L; E', L'; \mathbf{q}) dE dE' dL dL' = (2\pi\hbar)^{-3} \Delta_{if}(\mathbf{q}) dE dE' dL dL'$$

in terms of the phase-space integral

$$\Delta_{if}(\mathbf{q}) = \int d\mathbf{r} d\mathbf{p} \delta(H(\mathbf{r}, \mathbf{p}) - E) \delta(|\mathbf{L}(\mathbf{r}, \mathbf{p})| - L) \times \delta(H(\mathbf{r}, \mathbf{p} + \mathbf{q}) - E') \delta(|\mathbf{L}(\mathbf{r}, \mathbf{p} + \mathbf{q})| - L')$$

of δ functions involving states $i = (E, L)$ and $f = (E', L')$. For transitions between bound states the transition probability is obtained simply by the replacements $dE \rightarrow h\nu$ and $dL \rightarrow \hbar$. The integral can be recast in terms of the radial integral

$$\hat{R}_{if}(\mathbf{p}_1, \mathbf{p}_2; r) = \frac{1}{4\pi} \int_{-1}^1 \delta(rp_1 \sin \theta - L) \times d(\cos \theta) \int_0^{2\pi} \delta(rp_2 \sin \tilde{\theta} - L') d\phi, \quad (\text{B1})$$

where θ and $\tilde{\theta}$ are the angles between \hat{r} and \hat{p}_1 and \hat{p}_2 , respectively, as

$$\Delta_{if}(\mathbf{q}) = \int d\mathbf{p}_1 d\mathbf{p}_2 \delta(\mathbf{q} + \mathbf{p}_1 - \mathbf{p}_2) \delta(H(\mathbf{r}, \mathbf{p}_1) - E) \times \delta(H(\mathbf{r}, \mathbf{p}_2) - E') (4\pi \hat{R}_{if}(\mathbf{p}_1, \mathbf{p}_2; r) r^2 dr). \quad (\text{B2})$$

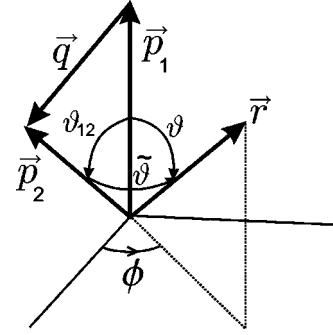


FIG. 13. The basic geometry for calculation of \hat{R}_{if} .

When \hat{R}_{if} is summed (integrated) over all L states, then $\int \hat{R}_{if} dL dL' = 1$ and

$$\int \hat{R}_{if} dL' = \frac{1}{2} \int_{-1}^1 \delta[rp_1 \sin \theta - L] d(\cos \theta) = L/(mr^2 p_1 \dot{r}). \quad (\text{B3})$$

1. Form factor for $EL \rightarrow E'L'$ transitions

Evaluation of \hat{R}_{if} for fixed L and L' is facilitated by noting, from Fig. 13, that

$$\cos \tilde{\theta} = \cos \theta_{12} \cos \theta + \sin \theta_{12} \sin \theta \cos \phi$$

in terms of $\hat{r}(\theta, \phi)$ and the fixed angle θ_{12} between \hat{p}_1 and \hat{p}_2 .

On changing the ϕ variable to $\tilde{\theta}$ in Eq. (B1), the ϕ integral, for θ fixed, is

$$\int_0^{2\pi} \delta(rp_2 \sin \tilde{\theta} - L') d\phi = 2 \int_{|\theta - \theta_{12}|}^{\theta + \theta_{12}} S^{-1}(\tilde{\theta}, \theta, \theta_{12}) \times \delta(rp_2 \sin \tilde{\theta} - L') d(\cos \tilde{\theta}).$$

The factor 2 originates from the fact that, as $\phi = 0 \rightarrow \pi \rightarrow 2\pi$, the range $(|\theta - \theta_{12}|, \theta + \theta_{12})$ in $\tilde{\theta}$ is covered twice. The function

$$S = \sin \theta_{12} \sin \theta \sin \phi$$

is expressed as a function of $\tilde{\theta}$ and θ variables by

$$S^2(\tilde{\theta}, \theta; \theta_{12}) = \sin^2 \theta \sin^2 \tilde{\theta} - (\cos \theta_{12} - \cos \theta \cos \tilde{\theta})^2.$$

Subsequent integrations are facilitated by noting that

$$\delta(F(x)) = \sum_n \frac{(x - x_n)}{|F'(x_n)|}, \quad F(x_n) = 0.$$

Hence

$$(\sin \tilde{\theta}) \delta(rp_2 \sin \tilde{\theta} - L') = \left[\frac{L'}{mp_2 r^2 \dot{r}'} \right] \sum_{i=1}^2 \delta(\tilde{\theta} - \tilde{\theta}_i),$$

where the roots, $\tilde{\theta}_1 < \pi/2$ and $\tilde{\theta}_2 = \pi - \tilde{\theta}_1$, are given by

$$\sin \tilde{\theta}_i = L'/rp_2, \quad \cos \tilde{\theta}_1 = -\cos \tilde{\theta}_2.$$

The ϕ integral therefore reduces to

$$\int_0^{2\pi} \delta[rp_2 \sin \tilde{\theta} - L'] d\phi = \left[\frac{L'}{mp_2 r^2 \dot{r}'} \right] \times [S_+^{-1}(\tilde{\theta}_1, \theta) + S_-^{-1}(\tilde{\theta}_1, \theta)],$$

where

$$S_{\pm}^2(\tilde{\theta}_1, \theta) = \sin^2 \theta \sin^2 \tilde{\theta}_1 - (\cos \theta_{12} \pm \cos \theta \cos \tilde{\theta}_1)^2.$$

Upon θ integration,

$$\begin{aligned} 4\pi \hat{R}_{\text{if}}(\mathbf{p}_1, \mathbf{p}_2; r) &= \left[\frac{2L'}{mp_2 r^2 \dot{r}'} \right] \int_{-1}^1 [S_-^{-1}(\tilde{\theta}_1, \theta) \\ &\quad + S_+^{-1}(\tilde{\theta}_2, \theta)] \delta(rp_1 \sin \tilde{\theta} - L) d(\cos \theta) \\ &= \left[\frac{2LL'}{m^2 p_1 p_2 r^4 \dot{r} \dot{r}'} \right] [S_-^{-1}(\tilde{\theta}_1, \theta_1) \\ &\quad + S_-^{-1}(\tilde{\theta}_1, \theta_2) + S_+^{-1}(\tilde{\theta}_1, \theta_1) \\ &\quad + S_+^{-1}(\tilde{\theta}_1, \theta_2)], \end{aligned}$$

where $\sin \theta_1 = \sin \theta_2 = L_1/rp_1$, and $\cos \theta_2 = -\cos \theta_1$. From these relations and from the above definitions of the S_{\pm} functions, then

$$S_-(\tilde{\theta}_1, \theta_1) = S_+(\tilde{\theta}_1, \theta_2),$$

$$S_-(\tilde{\theta}_1, \theta_2) = S_+(\tilde{\theta}_1, \theta_1),$$

with the result that the radial integral is

$$\begin{aligned} 4\pi \hat{R}_{\text{if}}(\mathbf{p}_1, \mathbf{p}_2; r) &= \left[\frac{4LL'}{m^2 p_1 p_2 r^4 \dot{r} \dot{r}'} \right] [S_+^{-1}(\tilde{\theta}_1, \theta_1; \theta_{12}) \\ &\quad + S_-^{-1}(\tilde{\theta}_1, \theta_1; \theta_{12})]. \end{aligned}$$

Upon \mathbf{p}_2 integration in Eq. (B2)

$$\hat{R}_{\text{if}}(\mathbf{p}_1; r) = \int \hat{R}_{\text{if}}(\mathbf{p}_1, \mathbf{p}_2; r) \delta(\mathbf{p}_2 - (\mathbf{p}_1 + \mathbf{q}_1)) d\mathbf{p}_2,$$

S_{\pm} are evaluated using the substitutions

$$\sin \theta = L/rp_1, \quad \cos \theta = m\dot{r}/p_1,$$

$$\sin \tilde{\theta} = L'/rp_2, \quad \cos \tilde{\theta} = m\dot{r}'/p_2,$$

and

$$\cos \theta_{12} = (p_1^2 + p_2^2 - q^2)/2p_1 p_2$$

to give, simply,

$$2p_1 p_2 S_{\pm}(\tilde{\theta}_1, \theta_1) = \sqrt{(q^2 - A_{\pm}^2)(B_{\pm}^2 - q^2)},$$

expressed in terms of the momentum-change limits

$$A_{\pm}^2 = m^2(\dot{r} \pm \dot{r}')^2 + (L - L')^2/r^2$$

and

$$B_{\pm}^2 = m^2(\dot{r} \pm \dot{r}')^2 + (L + L')^2/r^2.$$

The integral $\hat{R}_{\text{if}}(\mathbf{p}_1; r)$ is then

$$4\pi \hat{R}_{\text{if}}(\mathbf{p}_1; r) = \left[\frac{8LL'}{m^2 r^4 \dot{r} \dot{r}'} \right] [G_{\text{if}}^+(r, q) + G_{\text{if}}^-(r, q)], \quad (\text{B4})$$

where

$$G_{\text{if}}^{\pm}(r, q) = \frac{1}{\sqrt{(q^2 - A_{\pm}^2)(B_{\pm}^2 - q^2)}}.$$

Since

$$mr^2/2 = E - V(r) - L^2/2mr^2$$

holds for the initial and final states, the S , A , and B functions, and hence integral (B1), are all independent of \mathbf{p}_1 . The transition integral (B2) is then

$$\Delta_{\text{if}}(\mathbf{q}) = \int_0^{\infty} 4\pi \hat{R}_{\text{if}}(r, q) \Pi(r, q) r^2 dr, \quad (\text{B5})$$

where the only \mathbf{p} integral is

$$\Pi(r, q) = \int \delta(H(\mathbf{r}, \mathbf{p}) - E) \delta(H(\mathbf{r}, \mathbf{p} + \mathbf{q}) - E') d\mathbf{p}.$$

Hence

$$\begin{aligned} \Pi(r, q) &= 2\pi \int_0^{\infty} p^2 dp \delta[p^2/2m + V(r) - E] \\ &\quad \times \int_{-1}^{+1} \delta[pq \cos \theta/m - E' - E + q^2/2m] d(\cos \theta), \end{aligned}$$

where θ is the angle between \mathbf{p} and \mathbf{q} . There is only one root provided that

$$p \geq p_0 = m/q |E - E' + q^2/2m|.$$

The \mathbf{p} integrations therefore yield

$$\Pi(r, q) = \frac{2\pi m^2}{q} \Theta(r, q),$$

where Θ is the step function having a value 1 if $V(r) \leq E - p_0^2/2m$ is satisfied, and zero otherwise. The final expression for the classical transition probability density (13) for $E, L \rightarrow E', L'$ impulsive transitions is therefore

$$\begin{aligned} P(E, L; E', L'; \mathbf{q}) &= \frac{1}{(2\pi\hbar)^3} \frac{2\pi m^2}{q} \\ &\quad \times \int 4\pi \hat{R}_{\text{if}}(r, q) \Theta(r, q) r^2 dr, \end{aligned} \quad (\text{B6})$$

where \hat{R}_{if} is given by Eq. (B4). Hence

$$P(E, L; E', L'; \mathbf{q}) = \frac{16\pi LL'}{(2\pi\hbar)^3 q} \int_{\mathcal{R}} \frac{dr/r^2}{\dot{r}\dot{r}'} [G_{\text{if}}^+(r, q) + G_{\text{if}}^-(r, q)] \Theta(r, q).$$

For hydrogenic systems, the condition $V(r) \leq E - p_0^2/2m$ is satisfied for any q and all r within the radial region \mathcal{R} (cf. Fig. 3). Thus the step function Θ is always unity.

The probability of $n, l \rightarrow n', l'$ transitions due to an impulsive momentum change is then

$$P_{nl, n'l'}(q) = (h\nu_{nl})(h\nu_{n'l'}) \hbar^2 \times P(E_n, (l+1/2)\hbar; E_{n'}, (l'+1/2)\hbar; \mathbf{q}).$$

2. Form factor for $EL \rightarrow E'$ transitions

On using Eq. (B3) in Eq. (B6) the probability density for $E, L \rightarrow E'$ transitions is

$$P(E, L; E'; \mathbf{q}) = \frac{L}{\pi\hbar^3 q} \int_0^\infty (vr)^{-1} \Theta(r, q) dr,$$

where $v(r)$ is the speed along the initial trajectory. Since $p^2 = 2m[E - V(r)]$, integration over r may be replaced by p integration and $dr/v = dp/V'(r)$ so that

$$P(E, L; E'; q) = \frac{L}{\pi\hbar^3 q} \sum_j \int_{p_0}^\infty |\dot{r}_j V'(r_j)|^{-1} dp,$$

where r_j is the root of $p^2 = 2m[E - V(r)]$. In terms of the momentum distribution (A5), then

$$P(E, L; E'; q) = \frac{mL}{g_l \hbar q} \int_{p_0}^\infty \rho(E, L; p) 4\pi p dp,$$

which for bound nl states is in agreement with previous results [8,16,6].

The classical form factor for $nl \rightarrow n'$ transitions in hydrogenic systems is, in atomic units,

$$P_{nl, n'l'}(q) = \frac{2(2l+1)}{\pi q n'^3} \int_{p_{\min}}^{p_{\max}} \frac{n}{p} (1+n^2 p^2)^{-2} \times \left[1 - \left(\frac{L(1+n^2 p^2)}{2n^2 p} \right)^2 \right]^{-1/2} dp,$$

where the integration limits are given by two conditions: the integrand is real and $p \geq p_0 = |q^2 + 1/n'^2 - 1/n^2|/2q$.

3. Form factor for $E \rightarrow E'$ transitions

Using Eq. (B6) with $\hat{R}_{\text{if}} = 1$, the probability density for $E \rightarrow E'$ transitions is

$$P(E, E'; q) = \frac{2\pi m^2}{q(2\pi\hbar)^3} \left(\frac{4}{3} \pi r_*^3 \right),$$

where r_* is the largest r which satisfy the condition

$$p(r) = 2m[E - V(r)] \geq p_0 = \frac{m}{q} |E' - E - q^2/2m|.$$

This probability density is exact for all $V(r)$ and has a simple physical interpretation. The transition probability is given by $\mathcal{V} \Delta \mathbf{p} / (2\pi\hbar)^3$, which is the number of states in the ‘reaction’ volume $\mathcal{V} = 4/3\pi r_*^3$ multiplied by the volume of momentum space $\Delta \mathbf{p}$ consistent with energy conservation. The initial- final-state energy conservation equations are $E = p^2/2m + V(r)$ and $E' = E + \mathbf{q} \cdot \mathbf{p}/m + q^2/2m$, respectively. Then

$$\Delta \mathbf{p} = \int_{\phi=0}^{2\pi} d\mathbf{p} = 2\pi p^2 dp d(\cos \theta) = \frac{2\pi m^2}{q} dE dE',$$

where the z axis is along \hat{q} .

The classical form factor for $n \rightarrow n'$ transitions is

$$P_{nn'}(q) = (h\nu_n)(h\nu_{n'}) P(E_n, E_{n'}; q).$$

For Coulomb attraction $V(r) = -Ze^2/r$, then

$$r_*(q) = 8(Ze^2 m) q^2 [q^4 - 4m(E + E')q^2 + 4m^2(E - E')^2]^{-1}$$

so that the transition probability, with the substitution $q = Q(Z\hbar/a_0)$ now becomes

$$P_{n, n'}(Q) = \frac{2^9}{3\pi(nn')^3} Q^5 \left[Q^4 + 2 \left(\frac{1}{n^2} + \frac{1}{n'^2} \right) Q^2 + \left(\frac{1}{n^2} - \frac{1}{n'^2} \right)^2 \right]^{-3}.$$

APPENDIX C: CALCULATIONS OF QUANTAL FORM FACTORS

The quantal transition probability (5) for the hydrogen atom is in general a rational function of the momentum transfer q because Eq. (5) with $\Psi(\mathbf{r}) = R_{nl}(r)Y_{lm}(\hat{r})$ can be decomposed as

$$F_{nl, n'l'}(\mathbf{q}) = (2l+1)(2l'+1) \sum_{L=|l-l'|}^{l+l'} f_{n'l'}^L(q)^2 (2L+1) \times \begin{Bmatrix} L & l & l' \\ 0 & 0 & 0 \end{Bmatrix}^2$$

where $\{\dots\}$ is the Wigner $3j$ symbol, and $f_{n'l'}^L(q)$ is the radial integral:

$$f_{n'l'}^L(q) = \int_0^\infty R_{nl}(r) R_{n'l'}(r) j_L(qr) r^2 dr, \quad (\text{C1})$$

where j_L is the modified Bessel function. Because the radial wave function R_{nl} has the simple structure $e^{-r/n} r^l Q(r)$,

where Q is a polynomial of order $n-l-1$, integral (C1) contains only terms with the form

$$I_{k,L}(\alpha, q) = \int_0^\infty e^{-\alpha r} r^k j_L(qr) dr,$$

where α is $1/n + 1/n'$ and k is an integer number ($k = l + l' + 2, \dots, n + n'$) greater than L . This integral is the following rational function in q :

$$I_{k,L}(\alpha, q) = \frac{q^L \alpha^{k-L-1}}{(2L+1)(2L-1)!!} \frac{(L+k)!}{(\alpha^2 + q^2)^k} \times {}_2F_1\left(-\frac{k-L}{2} + 1, -\frac{k-L}{2} + \frac{1}{2}, L + \frac{3}{2}; -\frac{q^2}{\alpha^2}\right),$$

since the hypergeometric function ${}_2F_1$ is a polynomial when either the first or second argument is an integer. This proves that integral (C1), and hence the quantal form factor (14), are rational function in q . It also provides the practical procedure to calculate the quantal probability (14) in an analytical form.

The quantal transition probability (21) can be written in terms of the density matrix element, $\rho_n(\mathbf{r}, \mathbf{r}')$ = $\sum_{l,m} \psi_{nlm}^*(\mathbf{r}) \psi_{nlm}(\mathbf{r}')$, as

$$P_{nn'}(q) = \int \int d\mathbf{r} d\mathbf{r}' e^{iq\mathbf{r} \cdot \mathbf{r}'} \rho_n(\mathbf{r}, \mathbf{r}') \rho_{n'}^*(\mathbf{r}, \mathbf{r}').$$

The density ρ_n is the residue of the Coulomb Green's function [17] and can be calculated from

$$\rho_n(\mathbf{r}, \mathbf{r}') = \lim_{E \rightarrow E_n} (E - E_n) \mathcal{G}_E(\mathbf{r}, \mathbf{r}') = \frac{1}{\pi n a_0^3} \frac{P_n}{x - y}$$

in the spatial variables (x, y) given by

$$x = Z/a_0(r + r' + \rho), \quad y = Z/a_0(r + r' - \rho)$$

where $\rho = |\mathbf{r} - \mathbf{r}'|$. The function P_n has a simple structure. Because

$$P_n = \left(\frac{\partial}{\partial x} - \frac{\partial}{\partial y} \right) [M_{n,1/2}(x/n) M_{n,1/2}(y/n)],$$

where M is Whittaker's function, then P_n is simply $\exp[-(x+y)/2n] \times$ polynomial in x and y . Thus

$$P_n(x, y) = -\frac{e^{-(x+y)/2n}}{2n^3} [2n(x-y)f_n(x)g_n(x) + (n-1)xy(f_n(x)g_n(y) - g_n(x)f_n(y))],$$

where the polynomials

$$f_n(x) = {}_1F_1(1-n, 2, x/n), \quad g_n(x) = {}_1F_1(2-n, 3, x/n)$$

are given by the degenerate hypergeometric function ${}_1F_1$, where the first argument is a negative integer. Finally, $P_{nn'}$ is the integral in x, y variables:

$$P_{nn'}(q) = \frac{1}{24nn'} \int_0^\infty \int_0^\infty dx dy \sin(q(x-2)/2) \times (x^2 + 4xy + y^2) P_n(x, y) P_{n'}(x, y) / (x-y).$$

The observation that $P_n(x, x) = 0$, means that $x - y$ is a divisor for $P_n(x, y)$. On writing \sin in exponential form, the integral contains only primitive terms of the form $x^m(f \text{ or } g)(x) e^{-\alpha_\pm x}$, with various positive integer powers m and $\alpha_\pm = (1/n + 1/n' \pm iq)/2$. The elementary integrals

$$\int_0^\infty x^m f_n(x) e^{-\alpha x} dx = \left(\frac{\alpha n - 1}{\alpha n} \right)^n \frac{m!}{\alpha} \left(\frac{n}{\alpha n - 1} \right)^m \times {}_2F_1(n + 1, 1 - m, 2, 1/\alpha n)$$

and

$$\int_0^\infty x^m g_n(x) e^{-\alpha x} dx = \left(\frac{\alpha n - 1}{\alpha n} \right)^n \frac{m!}{\alpha} \left(\frac{n}{\alpha n - 1} \right)^m \times {}_2F_1(n + 1, 2 - m, 3, 1/\alpha n)$$

are rational functions in α which is linear in q . The form factor $P_{nn'}$ is therefore a rational function of q . The procedure described is remarkably efficient since it reduces the multiple integrations to a finite number of symbolic operations by (a) recognizing the primitive terms, and (b) replacing them with the appropriate elementary integrals. Based on this procedure, the results of calculations for the transition probabilities for $n' = 1, 2, 3, 4, 5$, and 6 and arbitrary n are presented in Table I. This illustrates the power of the method. The form factors for transitions from K, L , and M shells were obtained by Bethe and Walske [18]. The form factors for transitions to continuum states with wave number k are obtained by analytical continuation replacing n with i/k . The dipole oscillator strengths for $n - n'$ transitions,

$$f_{nn'} = 2\Delta E_{\text{a.u.}} \lim_{q \rightarrow 0} \frac{P_{nn'}(q)}{q^2},$$

can be readily deduced from the results presented in Table I.

- [1] M.T. Frey, F.B. Dunning, C.O. Reinhold, S. Yoshida, and J. Burgdörfer, *Phys. Rev. A* **59**, 1434 (1999).
- [2] See, e.g., N. F. Mott and H. S. W. Massey, *The Theory of Atomic Collisions* (Oxford University Press, London, 1965).
- [3] D. Vrinceanu and M. R. Flannery, *Phys. Rev. Lett.* **82**, 3412 (1999).
- [4] M. R. Flannery, in *Rydberg States of Atoms and Molecules*, edited by R. F. Stebbings and F. B. Dunning (Cambridge University Press, Cambridge, 1983), p. 393.
- [5] I. Bersons and A. Kulsh, *Phys. Rev. A* **55**, 1674 (1997); **59**, 1399 (1999).
- [6] I.L. Beigman and V.S. Lebedev, *Phys. Rep.* **250**, 95 (1995); V. S. Lebedev and I. L. Beigman, *Physics of Highly Excited Atoms and Ions* (Springer-Verlag, Berlin, 1998).
- [7] Y. Fang, A.N. Vasil'ev, and V.V. Mukhailin, *Phys. Rev. A* **58**, 3683 (1998).
- [8] F. Gounand and L. Petitjean, *Phys. Rev. A* **30**, 61 (1984).
- [9] L. Vriens, in *Case Studies in Atomic Collision Physics I*, edited by E. W. McDaniel and M. R. C. McDowell (North-Holland, Amsterdam, 1969), p. 364.
- [10] M.V. Berry, *Philos. Trans. R. Soc. London* **287**, 30 (1977); C.L. Mehta, *J. Math. Phys.* **5**, 677 (1964).
- [11] E.P. Wigner, *Phys. Rev.* **40**, 749 (1932).
- [12] V. Borodin, A.K. Kazanski, and V.I. Ochkur, *J. Phys. B* **25**, 445 (1992).
- [13] A.R. Filipelli, C.C. Lin, L.W. Anderson, and J.W. McConkey, *Adv. At., Mol., Opt. Phys.* **33**, 1 (1994); M.E. Lagus, J.B. Boffard, L.W. Anderson, and C.C. Lin, *Phys. Rev. A* **53**, 1505 (1996).
- [14] E. M. Lifshitz and L. P. Pitaevski, *Physical Kinetics* (Pergamon Press, Oxford, 1981), p. 104.
- [15] Inés Samengo, *Phys. Rev. A* **58**, 2767 (1998).
- [16] M. Matsuzawa, *Phys. Rev. A* **9**, 241 (1974).
- [17] L. Hostler, *J. Math. Phys.* **5**, 591 (1964).
- [18] H.A. Bethe, *Ann. Phys. (Leipzig)* **5**, 325 (1930); M.C. Walske, *Phys. Rev.* **101**, 940 (1956).